REPORT DOCUMENTATION PAGE

Form Approved
OMB No. 0704-0188

1. AGENCY USE ONLY (Leave blank)	2. REPORT DATE	3. REPORT TYPE AND DATES COVERED
	16 Apr 96	Translation

4. TITLE AND SUBTITLE
Laser-Interferometer with Phase Compensation

5. FUNDING NUMBERS
AFOSR Grant
F49620-94-1-0067

6. AUTHOR(S)
Author: G. Smeets and A. George, I.S.L., France.
Translated by Andreas Goetz, Purdue University

7. PERFORMING ORGANIZATION NAME(S) AND ADDRESS(ES)
Aerospace Sciences Lab.
3 Purdue University Airport
West Lafayette IN 47906-3371

8. PERFORMING ORGANIZATION REPORT NUMBER

9. SPONSORING/MONITORING AGENCY NAME(S) AND ADDRESS(ES)
Air Force Office Of Scientific Research
110 Duncan Avenue
Bolling AFB
Washington DC 20332-0001

10. SPONSORING/MONITORING AGENCY REPORT NUMBER

11. SUPPLEMENTARY NOTES
Translation of Report R136/75, Institute Franco-Allemand de Recherches de Saint-Louis, Dr. G. Smeets, Dec. 1975. Translated by Mr. Andreas Goetz at Purdue University, School of Aeronautics and Astronautics, October 1995. Translation was corrected by G. Smeets.

12a. DISTRIBUTION/AVAILABILITY STATEMENT
Unclassified unlimited per original source document

12b. DISTRIBUTION CODE

13. ABSTRACT *(Maximum 200 words)*

In the light path of a double-beam interferometer operated with continuous laser light a compensator is located. This is an electrically controllable, artificial phase object, which instantly compensates for any variations in path length caused by the object under observation. To achieve this, the change in voltage on the compensator is proportional to the change of the optical path length due to the event. The result of this is an analog signal of the event, which also follows optical path changes over several wavelengths, thus opening up new possibilities in laser-interferometry applications.
The first measurements with this method are being described, and the capabilities of a new kind of Doppler-interferometer are being discussed.

14. SUBJECT TERMS	15. NUMBER OF PAGES
Laser interferometer, gas dynamics	38 pages
	16. PRICE CODE

17. SECURITY CLASSIFICATION OF REPORT	18. SECURITY CLASSIFICATION OF THIS PAGE	19. SECURITY CLASSIFICATION OF ABSTRACT	20. LIMITATION OF ABSTRACT
UNCLASSIFIED	UNCLASSIFIED	UNCLASSIFIED	UL

Dr. G. Smeets - A. George
I.S.L.
5 Rue Du General Cassagnov
68301 Saint-Louis
FRANCE

Report
R136/75

Laser-Interferometer with Phase Compensation

Saint-Louis, Dec. 5, 1975

Chief Engineer
(Auriol)

Chairman at the BWB
(Dr. Schall)

Translated from German by

Andreas R. Goetz
School of
Aeronautics & Astronautics
Purdue University
West Lafayette, IN 47906, USA

W. Lafayette, Oct. 22, 1995

Abstract

In the light path of a double-beam interferometer operated with continuous laser light a compensator is located. This is an electrically controllable, artificial phase object, which instantly compensates for any variations in path length caused by the object under observation. To achieve this, the change in voltage on the compensator is proportional to the change of the optical path length due to the event. The result of this is an analog signal of the event, which also follows optical path changes over several wavelengths, thus opening up new possibilities in laser-interferometry applications.
The first measurements with this method are being described, and the capabilities of a new kind of Doppler-interferometer are being discussed.

Contents

Introduction

Interferometry allows for the determination of the optical path length ϕ of light rays:

$$\phi = \int n \cdot ds. \tag{1}$$

On the one hand, information about the refractive indices and parameters derived from them can be gained. This makes interferometric flow measurement feasible, for example. The other way round, geometrical path lengths and their changes - that is, motion - can be measured.

For many measurement problems the utilization of laser-interferometers (continuous beam + photo diode) yielded advantages. Since 1969, a laser-differential interferometer, set up with Wollaston prisms, has been employed in gas-dynamic measurements at the ISL, [1] [2] [3]. Due to its low sensitivity to vibrations a stable adjustment to a interference can be performed, such that small changes in the optical path ($\delta\phi \leq \lambda / 10$) are linearly transformed into proportional signal voltages.

In the following sections, a novel technique of phase compensation for laser-interferometer will be described, which makes it possible to adapt the well-established methods of laser-differential interferometry to other types of interferometer like Mach-Zehnder and Michelson, since it does not require high mechanical and thermal stability anymore. Furthermore, the restriction to small optical path length changes an be dropped. Therefore the range of applications of laser interferometry is enhanced by phase compensation in multifarious ways.

Measurement Principle

a) Phase Compensation

The principle of phase compensation is outlined in figure 1. In the optical path of the laser interferometer a compensator is located, being able to impose additional phase shift between both ray paths of the interferometer. After merging both rays, they are mixed by means of a suitable optical system such that they will produce complementary interferences on two photo diodes simultaneously (the one interference is the negative of the other). The electric current passing through both diodes is proportional to the respective intensity of the incident light. In the middle of a slope, both diodes receive the same light intensity. Thus, both currents are equal, which keeps charge and voltage on the capacitor C constant. If now the measured object causes a change in optical path difference, this equilibrium will be disturbed. The light intensity on one diode increases, while it decreases on the other one. This leads to a change in voltage at the capacitor connected to the high-impedance input of an amplifier.

The output of the amplifier is connected to the compensator, which generates an additional optical path difference proportional to the output signal, thus compensating for the path difference in the interferometer and restoring the equilibrium. The compensator responds to any variation in the optical path, which thus becomes measurable by recording the compensator voltage. Small changes in path length are detectable as well as changes over many wavelengths.

For the set-up of the phase-compensating laser-interferometer it is advantageous to use polarization optics (see figure 2). Both rays can be distinguished by their direction of polarization being perpendicular to each other. It then becomes possible to combine the interferometer and the compensator in an arbitrary succession without losing the identity of both rays.

The rays are mixed in a Wollaston prism adjusted at an angle of 45° towards their polarization directions such that the results are two complementary interferences.

b) Interferometer

Figures 3 to 5 show how to set up the most common types of interferometers - Mach-Zehnder, Michelson and differential interferometer - with polarization optics. To achieve equal intensity in both ray paths, the incoming laser beam has to be linearly polarized at 45°, or circularly polarized.
For the circular polarization, a $\lambda / 4$-plate is mounted in front of the interferometer. As need arises, additional optical components, e.g. lenses for accurate laserlight focussing, are installed in the ray path, which is not depicted in the schematic figures 3 to 5.

For a Mach-Zehnder arrangement, Foster prisms can be used, since they can separate and merge the polarized ray paths again as demonstrated in figure 3.

The Michaelson set-up (figure 4) can be realized by means of a double-sided Foster prism in combination with two $\lambda / 4$-plates.

The differential interferometer with Wollaston prisms (figure 5) separates the ray components after polarizing them and can therefore be set up in the usual manner.

c) Compensators

There are several possibilities for transforming the amplifier output signal into an additional optical path difference.

A Pockels cell can generate very fast changes. Nowadays, by exploiting the transversal Pockels effect, half wave voltages of only 200 V can be achieved. However, a trade-off

between amplitude and frequency bandwidth has to be found, since the frequency bandwidth of high voltage DC-amplifiers decreases with increasing output amplitude.

Optical path changes can also be generated by displacing mirrors utilizing piezoelectric translators. In the simplest case, the reference mirror of a Michelson-interferometer can be shifted in this manner (figure 4). Then the compensator is an integral part of the interferometer.

Another possibility for phase compensation is offered by a differential interferometer path geometry deflected on a small mirror, which in turn is oscillated by a fast moving-coil vibrator (figure 6). A distance a between the rays and a mirror oscillation amplitude angle φ result in a light ray deflection of 2φ and a change in optical path difference of:

$$\Delta\phi = 2a \cdot \varphi. \tag{2}$$

The deflected differential interferometer is mounted behind the actually measuring interferometer, with the image of the measured object focussed on the oscillating mirror, and the mirror in turn imaged to the photo diodes.

In the case of slow changes of the phase object, the compensation can take place by displacing a Wollaston prism with a magnetic coil.

Control circuitry

a) Control loops featuring piezoelectric translators

Due to the feedback via compensator, control systems come into play. The control circuit properties are essential for the operation of phase-compensating laser-interferometers and therefore are now inspected more closely. First, the case of phase compensation by a piezoelectric translator is being examined.

The charge Q and the voltage drop U of the capacitor C in figure 1 and figure 2 are related by the equation:

$$U = \frac{Q}{C}. \tag{3}$$

The charge Q is governed by the currents i_1 and i_2 through the photo diodes:

$$Q = \int (i_1 - i_2)dt. \tag{4}$$

Due to the complementary interferences and the linear relationship between the light intensities and electric currents (which is a property of PIN-photo diodes) the optical path difference $\Delta\phi$ and the currents are related by:

$$i_1 = i_{01} \cdot \cos^2\left\{\pi \cdot \frac{\Delta\phi}{\lambda}\right\}$$
$$i_2 = i_{02} \cdot \cos^2\left\{\pi \cdot \frac{\Delta\phi}{\lambda}\right\}. \tag{5}$$

The optical path difference consists of three components:

$$\Delta\phi = \Delta\phi_{Int} - \Delta\phi_{Obj} + \Delta\phi_{Tr}. \tag{6}$$

$\Delta\phi_{Int}$ is a constant value from interferometer pre-adjustment, $\Delta\phi_{Obj}$ is generated by the measured object and $\Delta\phi_{Tr}$ by the piezoelectric translator.

$\Delta\phi_{Tr}$ is proportional to the translator mirror displacement $x - x_0$. In the case of normal reflection:

$$\Delta\phi_{Tr} = 2(x - x_0). \tag{7}$$

The translator is capable of mechanical oscillations. Thus, the mirror position x is determined by the corresponding general differential equation:

$$m \cdot \ddot{x} + r \cdot \dot{x} + s(x - x_0) = K. \tag{8}$$

The Force K acting on the mirror is proportional to the Voltage U on the capacitor C, since the capacitor is connected to the amplifier input (amplification gain v), while the amplifier output is controlling the translator. The implicated assumption is a sufficiently wide DC-amplifier bandwidth. From this follows:

$$K = d \cdot v \cdot U; \tag{9}$$

The sensitivity of the piezoelectric translator is d / s (amount of displacement per voltage unit).

Merging the above equations (3) to (9) leads to the following differential equation determining $\Delta\phi_{Tr}$:

$$m \cdot \Delta\dddot{\phi}_{Tr} + r \cdot \Delta\ddot{\phi}_{Tr} + s \cdot \Delta\dot{\phi}_{Tr} = \frac{v \cdot d}{C}\left[i_{01} - i_{02} + (i_{01} + i_{02}) cos\left\{ \frac{2\pi}{\lambda}\left(\Delta\phi_{Int} - \Delta\phi_{Obj} + \Delta\phi_{Tr} \right) \right\} \right] \tag{10}$$

The condition for system equilibrium is described by:

$$\Delta\dddot{\phi}_{Tr} = \Delta\ddot{\phi}_{Tr} = \Delta\dot{\phi}_{Tr} = 0. \tag{11}$$

This condition is fulfilled, if:

$$\Delta\phi = \Delta\phi_{Int} - \Delta\phi_{Obj} + \Delta\phi_{Tr} = \frac{\lambda}{2\pi} \cdot \arccos\left\{ \frac{i_{02} - i_{01}}{i_{02} + i_{01}} \right\}. \tag{12}$$

If both photo diodes are identical ($i_{01} = i_{02}$) these will be the middle points of the interference slopes:

$$\Delta\phi = \frac{\lambda}{4} \pm n \cdot \frac{\lambda}{2} \qquad n = 0,1,2,\ldots \tag{13}$$

A stable equilibrium is existing at every second slope, for $i_{01} = i_{02}$ at:

$$\Delta\phi = \frac{\lambda}{4} \pm n \cdot \lambda \tag{14}$$

The interference slopes are almost linear in a wide range. In this range is valid with good approximation the differential equation resulting from an expansion of the cosine term at the point of equilibrium:

$$m \cdot \Delta\dddot{\phi}_{Tr} + r \cdot \Delta\ddot{\phi}_{Tr} + s \cdot \Delta\dot{\phi}_{Tr} = \mp\frac{2\pi \cdot d \cdot v}{\lambda \cdot C}\sqrt{(i_{01} + i_{02})^2 - (i_{01} - i_{02})^2} \cdot (\Delta\phi - \Delta\phi_0). \tag{15}$$

$\Delta\phi_0$ is the optical path difference corresponding to the equilibrium. The minus sign is valid for the stable equilibrium points.

Using the abbreviation:

$$A = \frac{2\pi \cdot d \cdot v}{\lambda \cdot C}\sqrt{(i_{01} + i_{02})^2 - (i_{01} - i_{02})^2} \cdot (\Delta\phi - \Delta\phi_0) \tag{16}$$

the control system equation is shortened to:

$$m \cdot \Delta\dddot{\phi}_{Tr} + r \cdot \Delta\ddot{\phi}_{Tr} + s \cdot \Delta\dot{\phi}_{Tr} = -A \cdot (\Delta\phi - \Delta\phi_0). \tag{17}$$

This equation determines the relevant properties of the control system. Before analyzing the stability, the following homogeneous equation has to be examined:

$$\Delta\dddot{\phi}_{Tr} + \frac{r}{m}\Delta\ddot{\phi}_{Tr} + \frac{s}{m}\Delta\dot{\phi}_{Tr} + \frac{A}{m}\Delta\phi_{Tr} = 0. \tag{18}$$

Applying the general solution $\Delta\phi_{Tr} = e^{kt}$ leads to the characteristic equation:

$$k^3 + \frac{r}{m}k^2 + \frac{s}{m}k + \frac{A}{m} = 0. \tag{19}$$

With the transformation:

$$k = y - \frac{r}{3m} \tag{20}$$

the characteristic equation is given the form:

$$y^3 + 3py + 2q = 0\,, \tag{21}$$

where

$$3p = -\frac{r^2}{3m^2} + \frac{s}{m} \tag{22}$$

and

$$2q = \frac{2r^3}{27m^3} - \frac{r \cdot s}{3m^2} + \frac{A}{m}\,. \tag{23}$$

If

$$q^2 + p^3 \geq 0, \tag{24}$$

and

$$u = \sqrt[3]{-q + \sqrt{q^2 + p^3}}$$
$$v = \sqrt[3]{-q - \sqrt{q^2 + p^3}} \tag{25),(26}$$

are the real roots, then the solutions of the reduced equation are:

$$\begin{aligned} y_1 &= u+v \\ y_2 &= -\frac{u+v}{2}+\frac{i}{2}\sqrt{3}(u-v) \\ y_2 &= -\frac{u+v}{2}-\frac{i}{2}\sqrt{3}(u-v) \end{aligned} \tag{27}$$

The control system will remain stable, if the real part of all three characteristic equation solutions k_1, k_2, k_3 are less or equal Zero, that is:

$$\mathrm{Re}\left(k_{1,2,3}\right) \le 0. \tag{28}$$

The following characteristic parameters are introduced:

Eigenfrequency:

$$\omega_0 = \sqrt{\frac{s}{m}} \tag{29}$$

Damping coefficient α:

$$\alpha = \frac{r}{2m\omega_0}, \tag{30}$$

Feedback coefficient G:

$$G = \frac{A}{s \cdot \omega_0}. \tag{31}$$

A discussion reveals, that k_1 is always <0, and that the condition $\mathrm{Re}\left(k_{2,3}\right) \le 0$ is only fulfilled if:

$$G \le 2\alpha\,. \tag{32}$$

If an oscillator has the critical (optimal) damping of

$$\alpha = \frac{1}{\sqrt{2}}, \tag{33}$$

the stability condition, that is the condition for the highest allowable feedback coefficient, will be:

$$G = \frac{4\pi \cdot d \cdot v \cdot i_0}{\lambda \cdot C \cdot s \cdot \omega_0} \leq 1.4 . \tag{34}$$

For the sake of simplicity, identity of the photo diodes has been assumed here ($i_{01} = i_{02} = i_0$).

The speed of the compensator in following changes of the object depends on the feedback level. In the case of a uniform change $\Delta\dot{\phi}_{Obj}$, it is

$$\Delta\dot{\phi}_{Tr} = \Delta\dot{\phi}_{Obj} \tag{35}$$

and, according to equation (17):

$$\Delta\dot{\phi}_{Tr} = -\frac{A}{s}(\Delta\phi - \Delta\phi_0). \tag{36}$$

On the other hand, the displacement from equilibrium $\Delta\phi - \Delta\phi_0$ may not exceed certain limits, since the system would not remain on its interference slope, but would jump to another. From an estimation, the limit can be assumed to be:

$$|\Delta\phi - \Delta\phi_0| < \frac{\lambda}{2\pi}. \tag{37}$$

It follows from this assumption that:

$$|\Delta\dot{\phi}_{Obj}| < \frac{A \cdot \lambda}{2\pi \cdot s} = \frac{G\omega_0\lambda}{2\pi}. \tag{38}$$

If the feedback level is adjusted, such that the system according to equation (32) just barely does not allow undamped oscillations,

$$G = 2\alpha \tag{39}$$

then $\Delta\dot{\phi}_{Obj}$ is restricted to

$$|\Delta\phi_{Obj}| < \frac{l \cdot w_0 \cdot a}{p} = 2a \cdot l \cdot u_0, \tag{40}$$

where υ_0 is the eigenfrequency of the oscillator.

A harmonic optical path difference oscillation from the object assumed:

$$\Delta\phi_{Obj} - \Delta\phi_{Obj,0} = Q \cdot \sin(2\pi\upsilon t) \tag{41}$$

it follows that:

$$\Delta\dot{\phi}_{Obj} = 2\pi \cdot \upsilon \cdot Q \cdot \cos(2\pi\upsilon t). \tag{42}$$

Because of equation (40), the product of frequency and amplitude must fulfill the condition:

$$\upsilon \cdot Q \leq \frac{\lambda \cdot v_0 \cdot \alpha}{\pi} \tag{43}$$

for the compensator being able to follow up.

The condition stated by equation (40) was derived for the special case of a constant $\Delta\dot{\phi}_{Obj}$. However, this assumption holds reasonably true for the rough estimation of the feasible frequency and amplitude range stated in equation (43).

Unfortunately, common piezoelectric translators feature only weak damping:

$$\alpha \leq 0.1. \tag{44}$$

Values for υ_0 and α together with amplitude values for commonly available translators are given - if known - in table 1.

b) Control system featuring oscillating mirror

A control loop including a mirror as deflector is completely analogous to the control circuit with a piezoelectric translator examined in the section above. Thus, the respective relationships are valid here.
$\Delta\phi_{Tr}$ is replaced by $\Delta\phi_{Sp}$. Instead of eqn. (7), the following equation is used:

$$\Delta\phi_{Sp} = 2a(\varphi - \varphi_0). \tag{45}$$

φ is the the instantaneous oscillation angle of the mirror deflecting the ray path of a differential interferometer (figure 6). a is the distance between the two differential interferometer ray paths.

Equations (8) and (9) become:

$$\Theta\ddot{\varphi} + b\dot{\varphi} + D\varphi = M, \qquad M = e \cdot v_{Sp} \cdot U. \tag{46),(47}$$

Here, v_{Sp} defines the ratio of the amplifier output current to input voltage. e / D is the oscillating mirror sensitivity, stated as angle covered per unit current.

The parameters A, ω_0, α and G are introduced in quite the same manner as above:

$$A = \frac{2\pi \cdot a \cdot e \cdot v_{Sp}}{\lambda \cdot c} \sqrt{\left(i_{01} + i_{02}\right)^2 - \left(i_{01} - i_{02}\right)^2}$$

$$\omega_0 = \sqrt{\frac{D}{\Theta}}$$

$$\alpha = \frac{b}{2\Theta\omega_0} \qquad (48),(49),(50),(51)$$

$$G = \frac{A}{D\omega_0}$$

The stability condition for a oscillating mirror with a damping coefficient α turns out to be:

$$G = \frac{4\pi \cdot a \cdot e \cdot v_{Sp} \cdot i_0}{\lambda \cdot C \cdot D \cdot \omega_0} \leq 2\alpha. \qquad (52)$$

Equation (40) is still valid as a restriction for the rate of change of the ray path due to the object, $\Delta\dot{\phi}_{Obj}$, where in this case υ_0 symbolizes the moving-coil vibrator eigenfrequency.

Table 1 contains data about the values of υ_0, α, and amplitudes of available deflection mirrors. The oil-damped Siemens moving-coil vibrators have a damping coefficient of $\alpha = 0.7$.

c) Control system featuring Pockels cell

The equations (3) to (5) are also valid here. In equation (6), the optical path difference due to the Pockels cell, $\Delta\phi_{Pz}$, appears as follows:

$$\Delta\phi = \Delta\phi_{Int} - \Delta\phi_{Obj} + \Delta\phi_{Pz}. \qquad (53)$$

$\Delta\phi_{Pz}$ is proportional to the high voltage U_h applied to the Pockels cell:

$$\Delta\phi_{Pz} = g \cdot U_h \qquad (54)$$

In the case of phase compensation with a Pockels cell, the high voltage amplifier is the slowest element. Assuming, that the high frequencies are limited by the time constant τ_0 as in the case of an RC-amplifier, the following differential equation relating the input voltage U (capacitor voltage) and the high voltage at the output U_h is applicable:

$$\tau_0 \cdot \dot{U}_h + U_h = v \cdot U. \tag{55}$$

v is the amplification factor. The time constant τ_0 and the upper frequency limit υ_0 (with a 3 dB output gain drop) are related by:

$$\tau_0 = \frac{1}{2\pi \cdot \upsilon_0}. \tag{56}$$

From eqn. (55), a differential equation to express $\Delta\phi_{Pz}$ can be derived (again by expansion of the cosine series at an equilibrium point):

$$\tau_0 \cdot \Delta\ddot{\phi}_{Pz} + \Delta\dot{\phi}_{Pz} = \mp \frac{\pi g v}{\lambda \cdot C} \sqrt{\left(i_{01} + i_{02}\right)^2 - \left(i_{01} - i_{02}\right)^2} \cdot (\Delta\phi - \Delta\phi_0). \tag{57}$$

Here, the general solution $\Delta\phi_{Pz} = e^{kt}$ for the homogeneous equation yields the following characteristic equation:

$$k^2 + \frac{1}{\tau_0} k + \frac{B}{\tau_0} = 0, \tag{58}$$

where the abbreviation:

$$B = \frac{\pi g v}{\lambda C} \sqrt{\left(i_{01} + i_{02}\right)^2 - \left(i_{01} - i_{02}\right)^2} \tag{59}$$

has been introduced.

The solutions are:

$$k_{1,2} = \frac{1}{2\tau_0} \left[-1 \pm \sqrt{1 - 4\tau_0 B}\right]. \tag{60}$$

The real part of $k_{1,2}$ is always negative. This means, that this control system retains its stability at any feedback level.

A uniform change $\Delta\dot{\phi}_{Pz}$ reduces eqn. (57) to:

$$\Delta\dot{\phi}_{Pz} = -B \cdot \left(\Delta\phi - \Delta\phi_0\right). \tag{61}$$

From this follows because of (35) and the condition (37):

$$\left|\Delta\dot{\phi}_{Obj}\right| < \frac{B \cdot \lambda}{2\pi}. \tag{62}$$

When again introducing a dimensionless feedback coefficient:

$$H = \frac{B}{2\pi\upsilon_0} = B \cdot \tau_0, \tag{63}$$

this finally gives:

$$\left|\Delta\dot{\phi}_{Obj}\right| < \lambda \cdot \upsilon_0 \cdot H. \tag{64}$$

In the case of a harmonic optical path difference oscillation due to the measured object in eqns. (41) and (42), the product of frequency and amplitude has to fulfill the following condition due to the restraint in (64):

$$\upsilon \cdot Q \leq \frac{\lambda\upsilon_0 H}{2\pi}. \tag{65}$$

Theoretically, H is not restricted in range. In practice, the order of magnitude of H will be unity. Again, equation (65) is to be perceived as a rough estimation of the obtainable range of frequency and amplitude. The properties of usually sold Pockels cells and of suitable amplifiers are listed in table 1.

Ranges of Frequency and Amplitude

a) Stabilization for small amplitudes

Since the rate of change of the optical path length due to the object, $\Delta\dot{\phi}_{Obj}$, is constrained according to (40) and (64), the frequency and amplitude of the oscillations allowable is constrained also, which is expressed in (43) and (65).

The bandwidth is maximized by directly measuring on the slope without compensation, where the signal is picked off at the resistance R in figure 2. Then, the only limit for the resolution in time is the characteristic time consisting of R and the capacity of the cables to the measuring device, which can be adjusted to be very small (10^{-8} s).

The relation between $\Delta\phi_{Obj}$ and the resistance voltage drop, U_R, is:

$$U_R = \pi \frac{R}{\lambda} \sqrt{\left(i_{01} + i_{02}\right)^2 - \left(i_{01} - i_{02}\right)^2} \cdot \Delta\phi_{Obj} \approx 2\pi \frac{i_0 \cdot R}{\lambda} \cdot \Delta\phi_{Obj} . \tag{66}$$

In this case the control system is used for stabilization against mechanical vibrations and temperature drift of the interferometer by setting a weak feedback level.

With a weak feedback, the optical paths in the compensator respond only slowly. In this case, only the first derivatives are relevant in equation (17) and (57) respectively. It can be concluded that a control system featuring a piezoelectric translator tends to reach equilibrium, that is the middle of the flank, with the time constant

$$\tau_{Tr} = \frac{s}{A} = \frac{1}{G \cdot \omega_0} = \frac{s \cdot C \cdot \lambda}{4\pi \cdot d \cdot v \cdot i_0} \tag{67}$$

In the case of a system including an oscillating mirror, the time constant is:

$$\tau_{Sp} = \frac{D}{A} = \frac{1}{G \cdot \omega_0} = \frac{D \cdot C \cdot \lambda}{4\pi \cdot a \cdot e \cdot v \cdot i_0}, \tag{68}$$

and for a set-up including a Pockel cell:

$$\tau_{Pz} = \frac{1}{B} = \frac{1}{H \cdot \omega_0} = \frac{C \cdot \lambda}{2\pi \cdot g \cdot v \cdot i_0}. \tag{69}$$

When picking off the signal directly on R, the optical path change to be measured has to be restricted to $\pm\lambda/10$. τ is to be set such, that temperature drifts and mechanical vibrations are being compensated, but the frequency spectrum of interest is not distorted.

b) Pockels cell for mediocre amplitudes

By using Pockels cells, optical path changes over several wavelengths can be detected, where the rate of change has to be within the limits set by equation (64).

If the optical path changes contain high frequency ranges with the compensator not being able to follow, but which do not have an amplitude greater than $\lambda/10$, a combined set-up consisting of direct measurement and measurement of the compensator voltage is recommended.

In this case, the high voltage applied to the Pockels cell and the voltage on the resistance R are linearly combined, that is, a suitable monitor voltage U_M from the high voltage

amplifier output is added to U_R. U_M is proportional to the optical path length change generated in the Pockels cell:

$$U_M = \frac{v_M}{g} \cdot \Delta\phi_{Pz}. \tag{70}$$

v_M is the ratio between measured monitor voltage and the high voltage applied to the Pockels cell. U_R is always proportional to the optical path difference, by which the system deviates from its equilibrium:

$$U_R = 2\pi \cdot \frac{i_0 \cdot R}{\lambda}\left(\Delta\phi_{Obj} - \Delta\phi_{Pz}\right). \tag{71}$$

If now R is adjusted, or v_M is set, such that

$$\frac{v_M}{g} = 2\pi \cdot \frac{i_0 \cdot R}{\lambda}, \tag{72}$$

then the sum of U_R and U_M is proportional to $\Delta\phi_{Obj}$:

$$U = U_R + U_M = \frac{v_M}{g} \cdot \Delta\phi_{Obj}. \tag{73}$$

The adjustment is feasible in a simple manner by means of a second Pockels cell. The optical path length difference is modulated by a square wave generator set to small amplitude output. The measured voltage $U = U_R + U_M$ has to show the square wave undistorted.

c) Mechanical compensation for high amplitudes

Using a piezoelectric translator or an oscillating mirror, higher path length changes can be compensated. However, their mechanical systems tend to be slower.

The high frequency component with an amplitude smaller than $\lambda/10$ cannot be taken care of in the same manner as in the case of a Pockel cell system by adding U_R. There is a relationship analogous to (70) existing:

$$U_R = 2\pi \frac{i_0 \cdot R}{\lambda}\left(\Delta\phi_{Obj} - \Delta\phi_{Tr}\right) \tag{74}$$

However, in this case there is no generally valid, linear relation between a monitor voltage U_M and the optical path length difference $\Delta\phi_{Tr}$ generated by the compensator analogous to (70), since the compensator will not follow up to the applied voltage oscillations

without inertia any more, if the frequencies of the oscillations are not substantially lower than its eigenfrequency υ_0.

By artificially limiting the amplifier bandwidth to $\upsilon_g << \upsilon_0$, an amplifier output signal U_a proportional to $\Delta\phi_{Tr}$ is feasible:

$$U_a = \frac{s}{2d}\Delta\phi_{Tr}. \tag{75}$$

When adjusting R such that the relationship

$$\frac{2\pi \cdot i_0 \cdot R}{\lambda} = \frac{s}{2d} \tag{76}$$

is fulfilled, the following equation is again applicable:

$$U = U_R + U_a = \frac{s}{2d}\Delta\phi_{Obj}. \tag{77}$$

The adjustment can take place using another Pockels cell and a square wave generator again. Equation (77) is valid for phase object motion with high frequency spectra up to an amplitude of about $\lambda/10$ when constraining the product of frequency and high amplitudes $\upsilon \cdot Q$ by:

$$\upsilon \cdot Q \leq \frac{\lambda \upsilon_g H}{2\pi}, \tag{78}$$

where in the case of a piezoelectric translator with limited amplifier bandwidth υ_g the feedback level is given by:

$$H_{Tr} = \frac{2 \cdot d \cdot v \cdot i_0}{\lambda \cdot C \cdot s \cdot \upsilon_g}. \tag{79}$$

d) Dual control systems

For the measurement of phase objects of high frequency and amplitudes there is the possibility of using the combination of a Pockels cell and a mechanical compensator.

To achieve this, both systems are coupled by a suitable resistance R_2 as depicted in figure 7. Both compensators are optically switched in series. Both parts of the system are set up and dimensioned as described above. R_2 has to be chosen to increase the time constant R_2C_1 to substantially bigger values than the Pockels cell control loop characteristic time τ_{Pz}:

$$R_2 C_1 >> \tau_{Pz} = \frac{C_1 \cdot \lambda}{2\pi \cdot g \cdot v_{Pz} \cdot i_0} \tag{80}$$

Changes with a steep slope are compensated by the Pockels cell at first. Beyond this, the compensation is taken over by the mechanical compensator to the degree, to which the charge of C_1 is spilling over to C_2. Since the order of magnitude of C_1 is nF, while C_2 is of the order of μF to ensure the stabilization of the mechanical system, then $C_2 >> C_1$, that is, the charge of C_1 for the most part transfers to C_2.

When limiting the mechanical control system bandwidth not by the oscillator but artificially by the amplifier, then $\Delta\phi_{Obj}$ is given by a linear combination of voltage on the resistance R_1, U_{R_1}, Voltage U_h applied to the Pockels cell, and the mechanical system amplifier output U_a:

$$\Delta\phi_{Obj} = \frac{\lambda}{2\pi \cdot i_0 \cdot R_1} U_{R_1} + g \cdot U_g + \frac{2d}{s} U_a \tag{81}$$

U_{MPz} and U_{MTr} are the monitor voltages on both amplifier outputs, where:

$$\begin{aligned} U_{MPz} &= v_{MPz} \cdot U_h \\ U_{MTr} &= v_{MTr} \cdot U_a \end{aligned} \tag{82}$$

Then the sum

$$U = U_{R_1} + U_{MPz} + U_{MTr} \tag{83}$$

can be made proportional to $\Delta\phi_{Obj}$ by adjusting R_1, v_{MPz} and v_{MTr}:

$$\frac{\lambda}{2\pi \cdot i_0 \cdot R_1} = \frac{g}{v_{MPz}} = \frac{2d}{s \cdot v_{Mtr}}. \tag{84}$$

The adjustment in the manner described above by using a artificial phase object with a square-wave oscillation, created with a square wave generator and a second Pockels cell, has also been established here as well-behaved.

By shorting the circuit on capacitor C_2 the system is initialized into the middle of the compensation range.

With this combined system, phase objects exhibiting extremly fast variations (Mhz) at amplitudes of up to about $\lambda/10$ can be detected, furthermore frequencies in the mediocre range (10 kHz - 100 kHz) at a few λ, and slow variations over many λ.

First Tests and Applications

a) Ultrasonic wave measurement

Figure 8 shows an arrangement, by which ducted ultrasonic waves were measured. Using an ionophone (electrically modulated gas discharge), short ultrasonic wave trains were generated. These propagate as almost planar waves in a slightly divergent tube where they deform. This deformation, due on the one hand to absorption of high frequency content and on the other hand to steepening because of nonlinear acoustic effects at the finite amplitudes in the mbar-range, is to be examined.

As a measurement device, a Michelson arrangement featuring piezoelectric translator stabilization was chosen. Here, the optical path variations remain below $\lambda/10$. One of both interferometer legs intersects the tube perpendicular to its axis. In this leg the laser beam was focussed on about 0.2 mm diameter, so that its spatial resolution suffices for planar sonic waves of up to 500 kHz.

The advantage of this optical microphone is its capability of reproducing even those extremly high frequencies undistorted, that is, the signals follow up the pressure variations at the locus of the laser beam without phase delay. As an example, figure 8 shows the laser-interferometer signal trace of a disturbance generated by a short wave train of 100 kHz. For comparison, the signal trace of an ultrasonic wave condenser microphone installed in the tube wall was recorded on the same plot.

With a similar laser-interference microphone the signals stemming from the ultrasonic field in the proximity of a hot supersonic free jet generated by a shock tube have been measured. In this case, the ray path arrangement was of the Mach-Zehnder type, with the compensation being taken over by a Pockels cell. To achieve a measuring point locally defined as well as possible, the measuring laser beam was exposed to the sonic field only over a short distance, while its rest was shielded by small-diameter glass tubes closed at both ends with 0.1 mm thick glass plates. For maximization of the resolution in time the laser beam in the measuring section was focussed on some 10th of a millimeter, furthermore, the measuring section was adjusted parallel to the wave fronts. Figure 9 demonstrates this. The arrow points to the approximate location of the measurement point. The resolution in time turned out to be about 1 µs (5 data points of the signal were digitally recorded within 1 µs), which appears to be sufficient to show the existence of shock waves (steep slopes).

b) Measurement of small optical path length variations in a turbulence

The arrangement as it was used for the measurement of planar ultrasonic waves can in general be employed for the recording of any path variation with small amplitudes. Currently, a stabilized Mach-Zehnder interferometer is being operated at the ISL to

determine the second derivative of optical paths, $\partial^2\phi / \partial t^2$, in a turbulent structure. The optical path arrangement can as well be dubbed a modified Schlieren system, which allows for the simultaneous measurement of $\partial^2\phi / \partial x^2$ and $\partial^2\phi / \partial y^2$. In this way, d'Alembert's equation of the optical path

$$\phi = \frac{\partial^2\phi}{\partial t^2} + a^2\left(\frac{\partial^2\phi}{\partial x^2} + \frac{\partial^2\phi}{\partial y^2}\right), \tag{85}$$

which is responsible for emitting sound, can be determined in a turbulent structure.

c) Doppler interferometer

When setting up a dual-beam laser interferometer with a substantial difference in the length of both ray paths - when $\Delta\phi$ is large enough - it becomes highly sensitive to variations in wavelength $\Delta\lambda$, the interferometer becomes some kind of spectrometer. This idea appears to be straightforward when examining equation (5) for the sensor currents. A change in I_1, I_2 does not only result from an optical path difference $\Delta\phi$, but also from a change in wavelength λ, while $\Delta\phi_0 \neq 0$ and constant. Considering $\lambda = \lambda_0 + \Delta\lambda$, then:

$$\pi\frac{\Delta\phi_0}{\lambda} = \pi \cdot \Delta\phi_0 \cdot \frac{1}{\lambda_0 + \Delta\lambda} \approx \pi\frac{\Delta\phi_0}{\lambda_0}\left[1 - \frac{\Delta\lambda}{\lambda_0}\right] = \frac{\pi}{\lambda_0}\left[\Delta\phi_0 + \Delta\tilde{\phi}\right], \tag{86}$$

where

$$\Delta\tilde{\phi} = -\frac{\Delta\phi_0}{\lambda_0}\Delta\lambda. \tag{87}$$

With the introduction of this virtual path difference variation, $\Delta\tilde{\phi}$, the complete set of equations developed above can be applied again by simply replacing $\Delta\phi_{Obj}$ with $\Delta\tilde{\phi}$. Equation (87) shows that the sensitivity to wavelength variations increases with increasing $\Delta\phi_0$.

The sensitivity achievable is large enough to enable the measurement of small Doppler shifts. The relationship between the wavelength shift $\Delta\lambda$ of laser light with wavelength λ_0 reflected on a reflector or scattered on seed particles, and the reflector or particle velocity v is:

$$\frac{\Delta\lambda}{\lambda_0} = \frac{v}{c} \cdot 2\cos\frac{\beta}{2} \cdot \cos\gamma \tag{88}$$

According to figure 10, β is the angle between incident and measurement direction, and γ is the angle between the direction of motion and the bisection angle of incident and measurement direction. With normal reflection, the relationship simplifies to:

$$\left|\Delta\tilde{\phi}\right| = \left|\Delta\phi_0\right| \cdot \frac{2v_n}{c}, \tag{89}$$

where v_n is the normal velocity component of a reflector or scattering body and the measured virtual optical path length change $\Delta\tilde{\phi}$.

Almost all lasers in use - mono-mode lasers with very low power excepted - possess several axial modes. The emitted laser light spectrum therefore exhibits several sharp lines with equidistant wavelength difference $\Delta\lambda_0$, where:

$$\Delta\lambda_0 = \frac{\lambda^2}{2L}. \tag{90}$$

With a large $\Delta\phi_0$, the interferences for the different modes are not in phase any more, which can be seen in equation (5), when plugging in $\lambda, \lambda+\Delta\lambda_0, \lambda+2\Delta\lambda_0$ and so on. This results in diminishing contrast and also in generating undesired signal superpositions, since the distribution of the total intensity on all modes varies with time.

This noise generation can be avoided when choosing $\Delta\phi_0$ to be twice the laser resonator length L:

$$\Delta\phi_0 = 2L. \tag{91}$$

This gives:

$$\pi \frac{\Delta\phi_0}{\lambda + n \cdot \Delta\lambda_0} \approx \pi \frac{\Delta\phi_0}{\lambda} - n\pi \tag{92}$$

that is, the signal components are in phase again for all wavelengths.

Having unequal lengths of the two ray paths, the geometry of both ray bundles is most likely different from each other after merging them. In-phase interference is only achievable with parallel light bundles, that is, with very small aperture angle. The illumination strength of this arrangement as a spectrometer becomes very poor. It turns out that this problem can be addressed as well. In a Michelson interferometer, for instance, the mirror of the longer leg can be imaged by a telecentric system (two lenses the distance f_1+f_2 apart) onto a reference plane, which sits as far away from the division plate as the mirror belonging to the shorter path. Then the light bundle of the longer path is reflected virtually on the reference plane, and both reflected bundles possess identical geometry after merging them.

Figure 11 outlines a preliminary experiment for the test of this Doppler interferometer. The optical arrangement is a Michelson interferometer featuring a follow-up loop with a piezoelectric translator. The Doppler shift is generated by a small piston driven by pressurized air. The laser beam is reflected by a triplet mirror built into the piston face and after this sent back to the interferometer. First, the recording shows an almost linear increase in piston velocity up to the point, where the piston passes a ventilation orifice in the cylinder wall. Then, it is decelerated by an air cushion, and finally brought to negative speed. Further development implicated, some possible applications for the wavelength sensitive interferometer lie in the field of spectroscopy, in the velocity measurement of surfaces and bodies in motion - e.g. in the area of ballistics - and local velocity measurement in fluids and gases by means of transported seed particles. Because of its special application profile, the measurement techique described above might be able to support the well-established methods in those areas.

In the field of spectroscopy, the interferometer is capable of competing with the Fabry-Perot device. Used as a spectrometer, it can reach the extraordinarily high resolution of 10^8 to 10^9. Its decisive advantage over the Fabry-Perot device is its substantially higher illumination strength. It could be employed where the smallest of changes in time of a single spectral line are to be detected.

In the area of ballistics, the interferometer can register small amplitudes of motion also, in opposite to Radar-Doppler measurements. Since a signal proportional to velocity is generated directly, an increase in the measurement accuracy might be possible in some problems. Compared to the common Laser-Doppler methods, the spectroscopic methods allow for the measurement of velocities without upper limit. In comparison to Doppler diference methods the capability of measuring velocity components in the direction of the incident light might yield an advantage.

A comparison with laser anemometers commonly used in fluid mechanics reveal similarities. The local fluid velocity measurement takes place only indirectly via seed particles in both cases. The absence of an upper velocity limit, the yield consisting of a continuous analog signal of the velocity, the capability of measuring a velocity component in the direction of the incident light and the arbitrarily high number of seed particles allowable in the test volume might turn out to be an advantage. The latter feature enables measurements in turbid fluids and suds.

In order to measure absolute velocities, the laser resonator has to be stabilized by a piezoelectric translator with a Fabry-Perot etalon coupled to it as a wavelength normal. Without stabilization, the laser wavelength is prone to a slow drift due to thermally related changes of the laser resonator.

d) Measurement of optical path oscillations of higher order of magnitude with dual-control device

To record larger optical path variations with high frequency content, a dual control loop was arranged according to the principle outlined in figure 7. A Pockels cell is combined with an oscillating mirror as a mechanical compensator. The precise data of the system are as follows:

1. Control loop with deflecting mirror

Reflecting mirror:	Siemens S 2000 T with
	$\omega_0 = 2\pi \cdot 2000\ s^{-1}$
	$\alpha = 0.7$
	$e/D = 6\ A^{-1}$
Ray distance:	$a = 0.025$ cm
Amplitude of current:	$i_0 = 2.5 \cdot 10^{-4}$ A
Capacitor:	$C_2 = 0.5\ \mu F$
Amplifier:	Tektronix P 6045 FET Probe + 10 x Attenuator
	$v_{Sp} = 8.33 \cdot 10^{-4}$ A/V.

This gives a feedback level of $G = 1$ and a time constant of $\tau_{Sp} = 8 \cdot 10^{-5}$ s.

2. Control loop with Pockels cell

Pockels cell:	Microphysic XP 2 with
	$g = \lambda/400\ V^{-1}$
Amplitude of current:	$i_0 = 0.25 \cdot 10^{-4}$ A
Capacitor:	$C_1 = 1.5$ nF
Amplifier:	Electro-Optic Developments LA 10 A
	with first-stage amplifier in Tektronix 3A9-slide in,
	$v_{Pz} = 167$.

This gives a characteristic time of $\tau_{Pz} = 2.3 \cdot 10^{-6}$ s.

3. The rest of the system data are:

Coupling resistance R_2:	10 kΩ, variable
Resistance R_1:	1 kΩ, variable
Diodes:	2 x HP 5082-4207
DC-Voltage source:	2 x 4.5 V flashlight battery.

After adjustment as given in equation (84), the sum of the signals as in equation (83) is generated. For the test of the system, optical path length variations in turbulent welding torch flames over several wavelengths were recorded. The figures 12 and 13 show samples of such recordings.

In the near future, the system is planned to be utilized for the examination of strong ultrasonic waves radiated by supersonic free jets.

Literature

G. Smeets,
4-Ray-Laser-Interferometer for Measurements on fast-changing Weak Phase Objects.
ISL - T - 21/70

G. Smeets, A. George,
Gas-Dynamic Investigations in a Shock Tube using a highly sensitive Laser-Interferometer.
ISL - 14/71

G. Smeets, A. George,
Applications of the Laser-Differential Interferometer in Gas Dynamics.
ISL - 28/73

System	ν_0	α	Sensitivity	Amplitude	Remarks
Piezoelectric Translator			d/s	Δx	
Eldon MD 20	12 kHz	< 0.1	$2 \cdot 10^{-6}$ mm/V	$4 \cdot 10^{-3}$ mm	
Physics Instruments P-0084			$2 \cdot 10^{-5}$ mm/V	$2 \cdot 10^{-2}$ mm	
Deflecting Mirror			e/D	$\Delta\varphi$	Due to mirror dimensions:
Siemens S 2000 T	2 kHz	0.7	6 A^{-1}	$\pm$ 0.46	$a \leq 0.3$ mm
Siemens S 10 000 T	10 kHz	0.7	0.7 A^{-1}	$\pm$ 0.05	$a \leq 0.3$ mm
General Scanning G-0612	2.1 kHz	< 0.1	0.14 A^{-1}	$\pm$ 0.10	$a \leq$ 4 mm
Pockels Cell			(λ = 6328 Å)		
Microphysic XP 2			420 V/λ	$\pm$ 1000 V	
Coherent Radiation Mod. 20			230 V/λ	$\pm$ 500 V	
Amplifier					
Electro Optic Developments					
LA 10 A	500 kHz			0 - 1500 V	
Optimation PA 25 A	2 MHz			$\pm$ 500 V	

Table 1

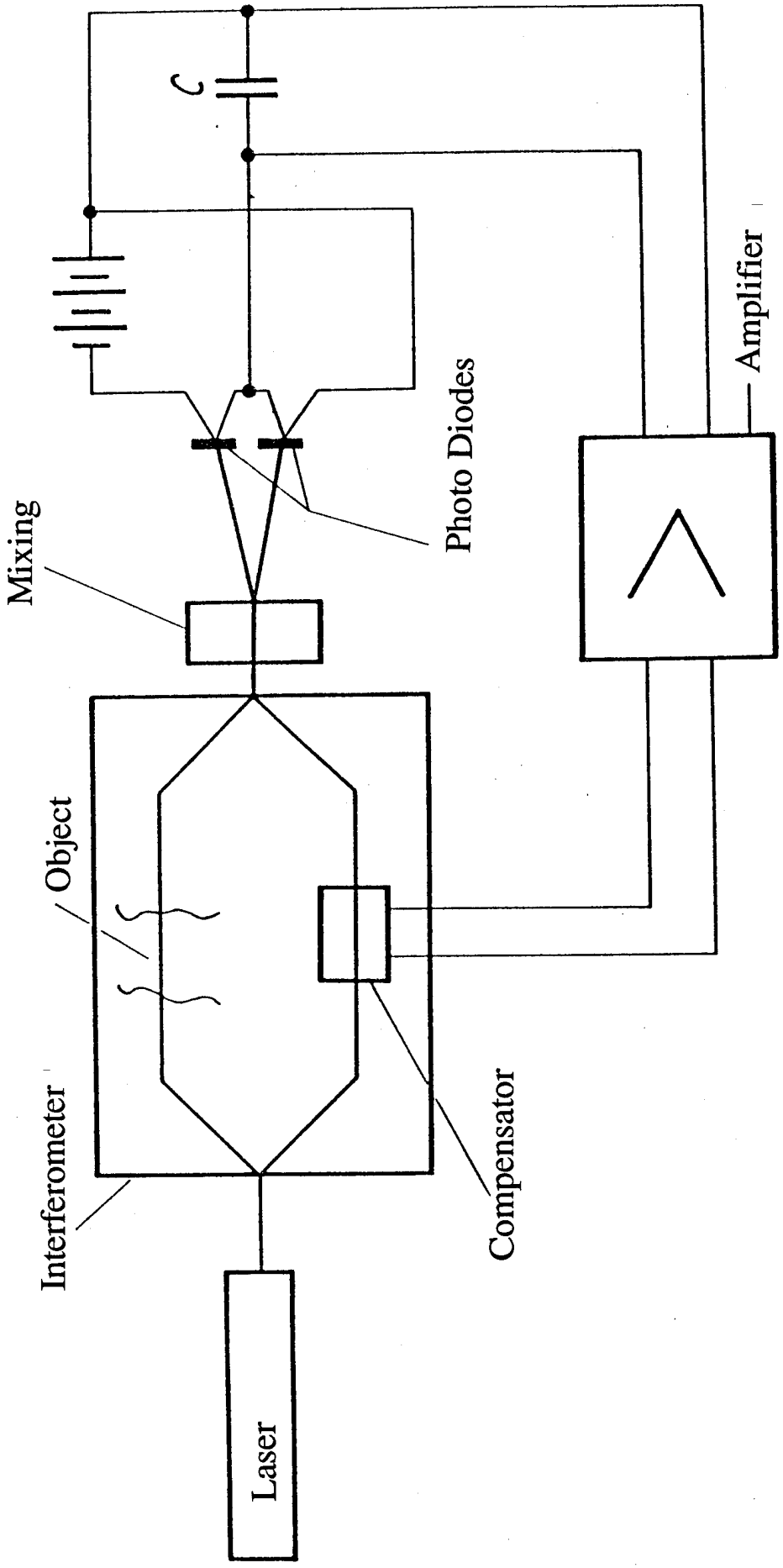
C
Amplifier
Photo Diodes
Mixing
Object
Interferometer
Compensator
Laser

Fig. 1

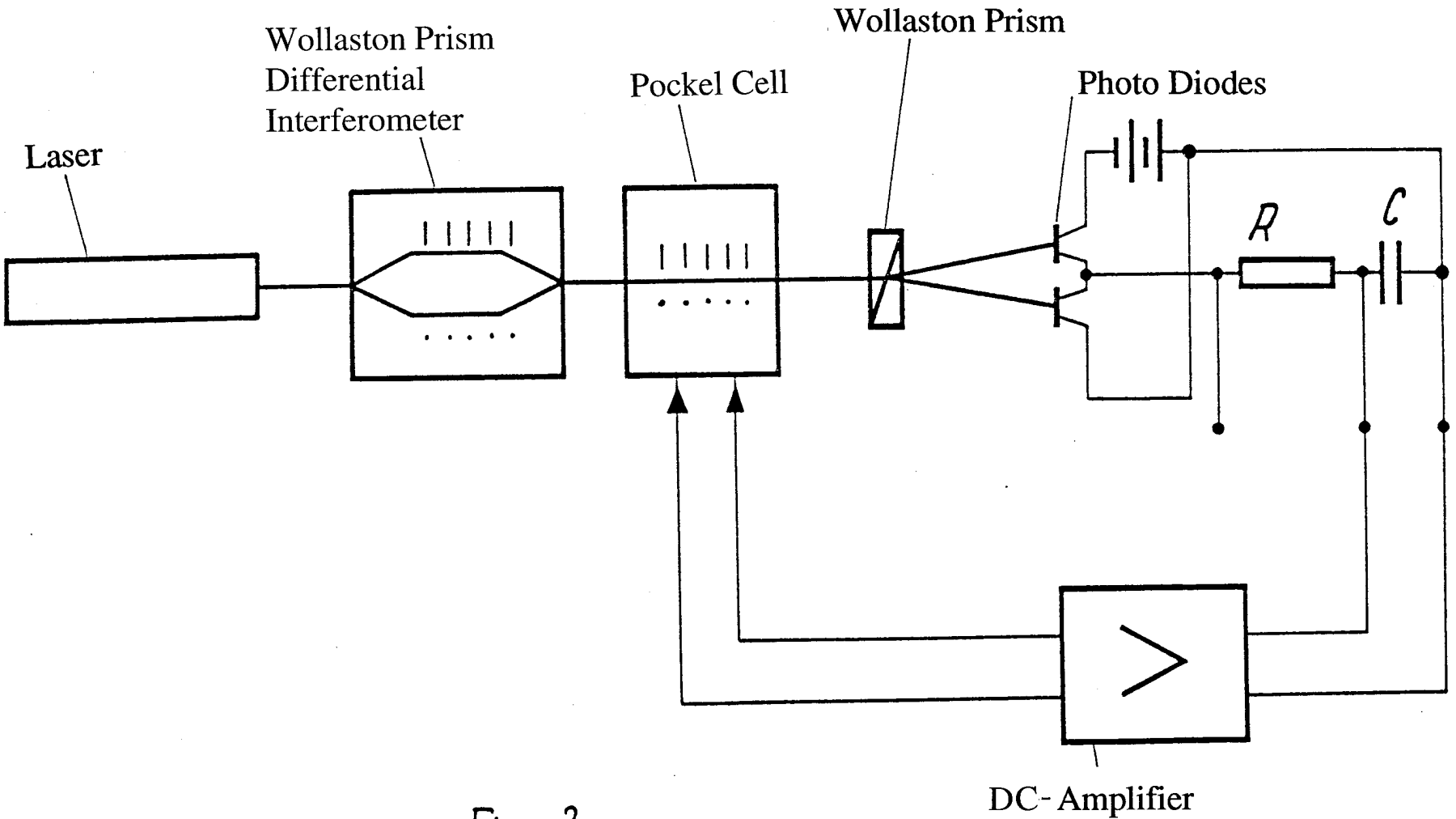
Wollaston Prism
Differential
Interferometer
Pockel Cell
Wollaston Prism
Photo Diodes
Laser
R
C
DC- Amplifier

Fig. 2

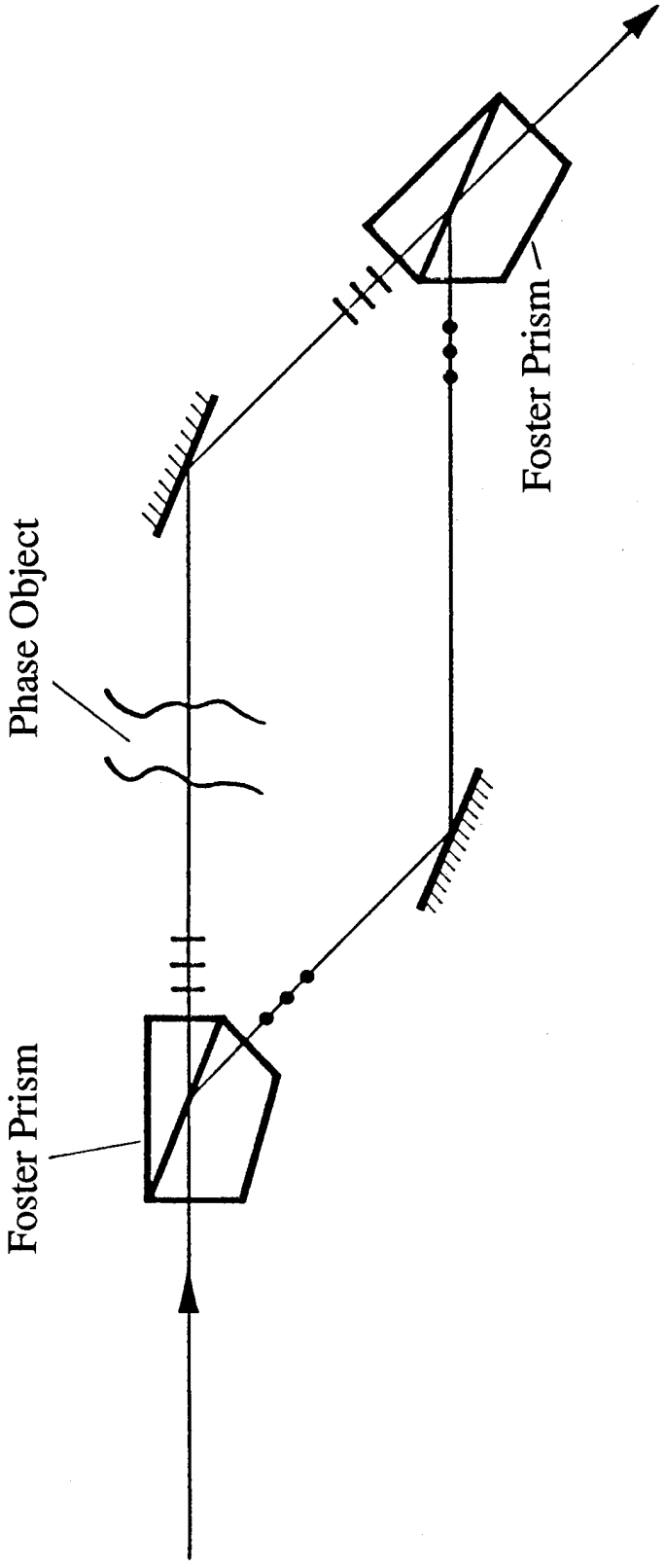

Fig. 3

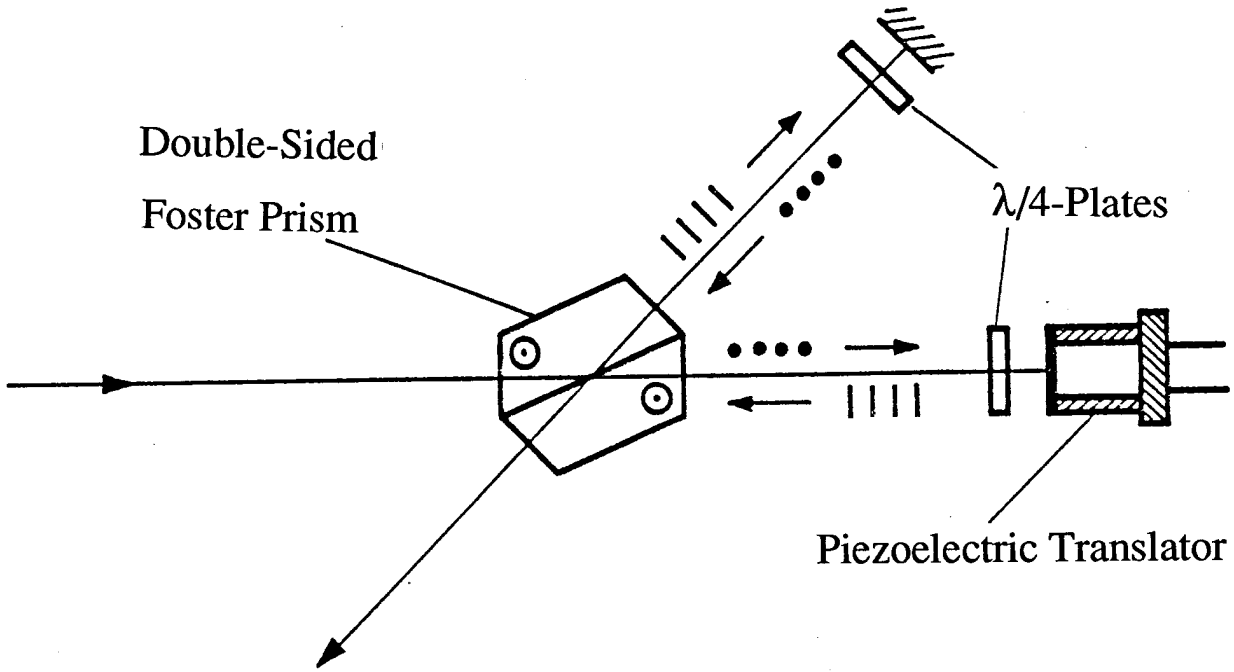
Double-Sided
Foster Prism
λ/4-Plates
Piezoelectric Translator

Fig. 4

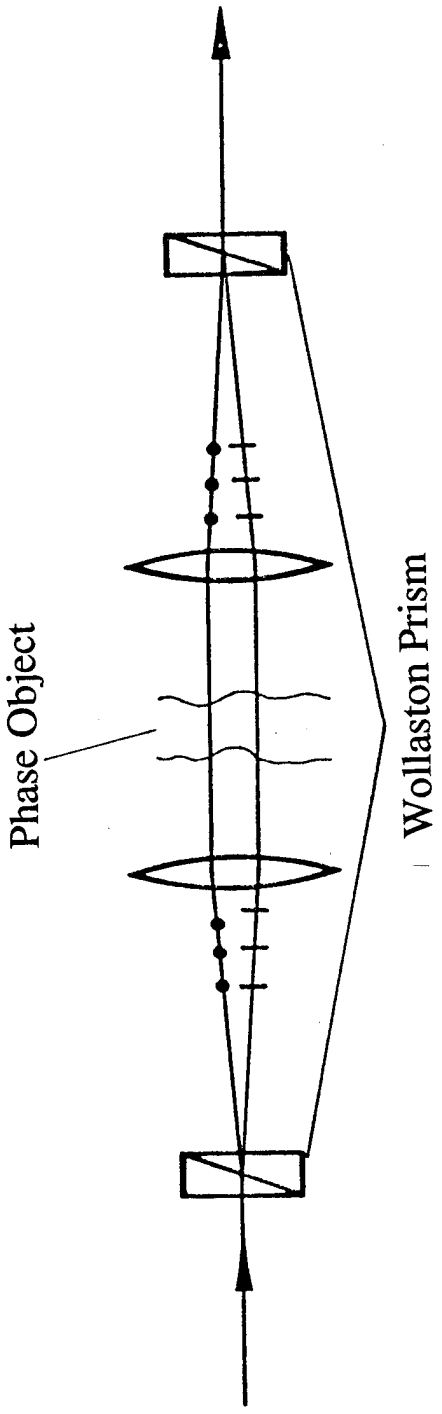

Fig. 5

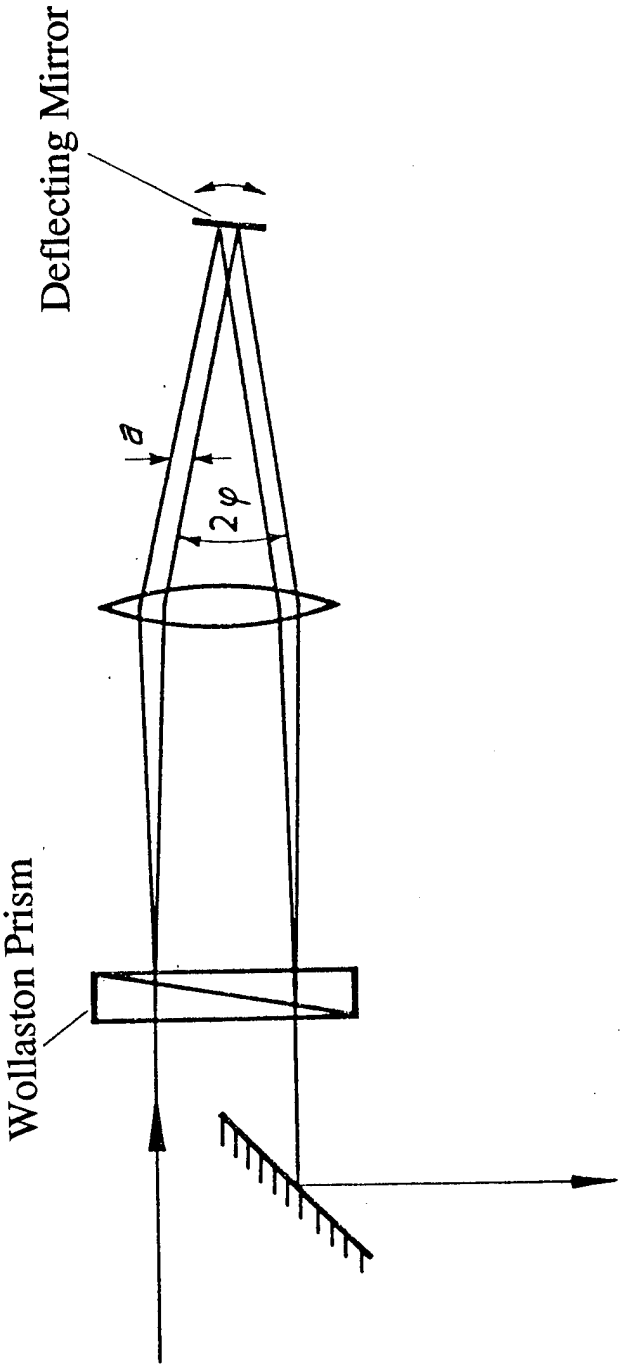

Fig. 6

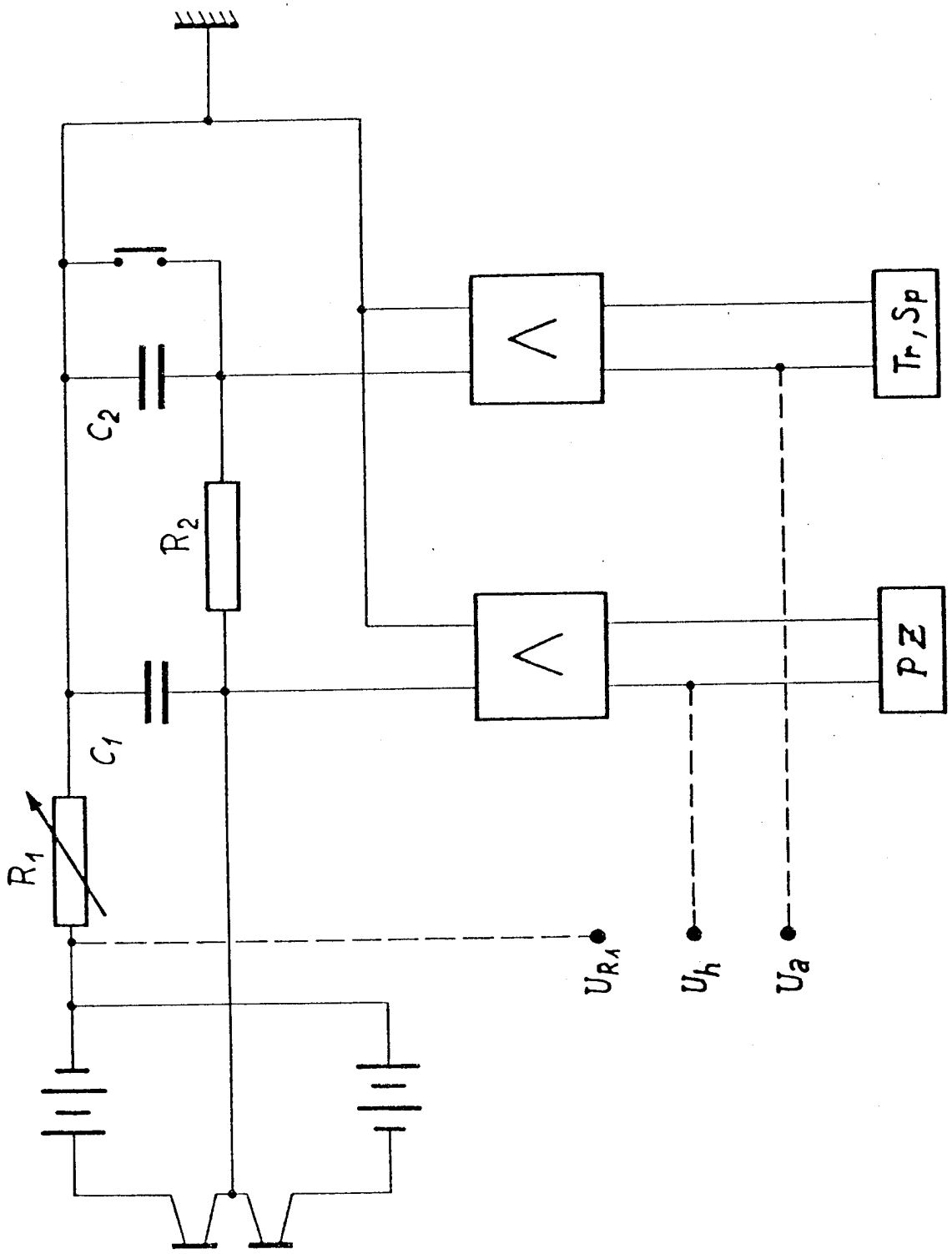

Fig. 7

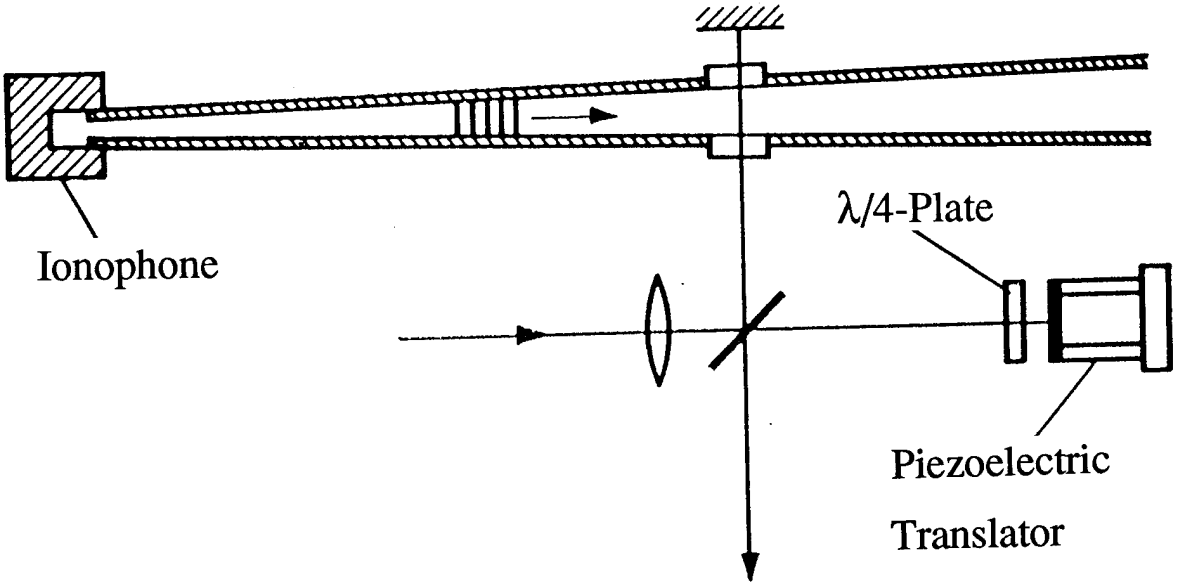
Ionophone
λ/4-Plate
Piezoelectric
Translator

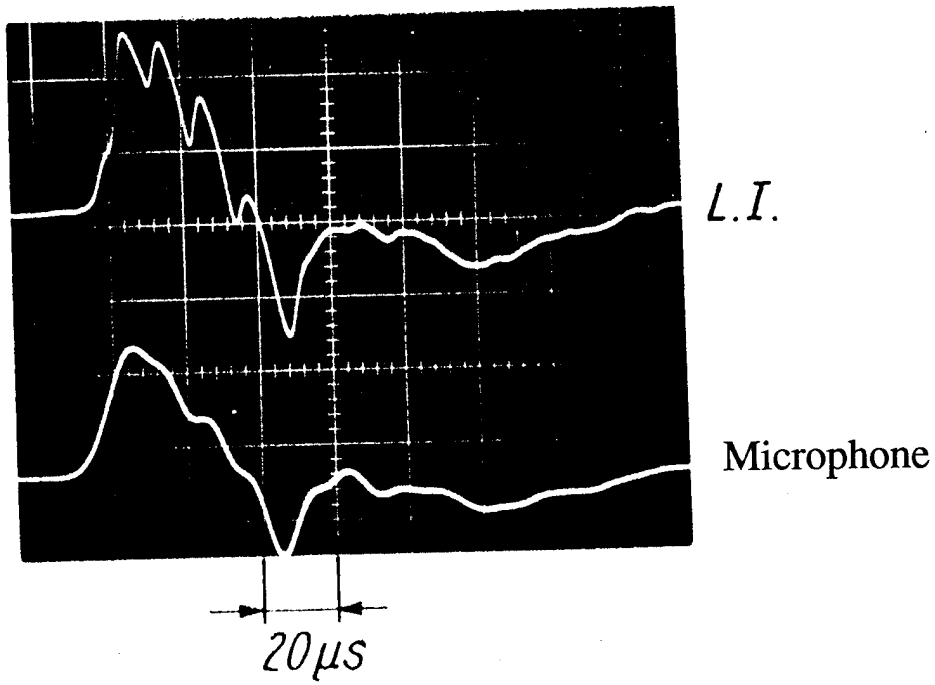
L.I.
Microphone
20μs

Fig. 8

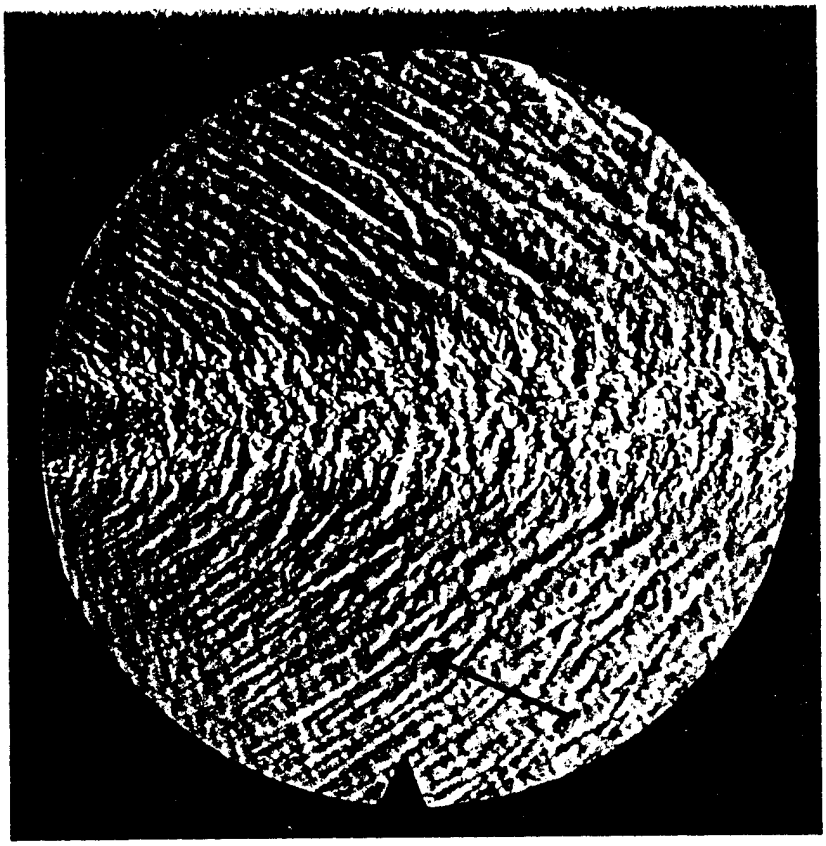

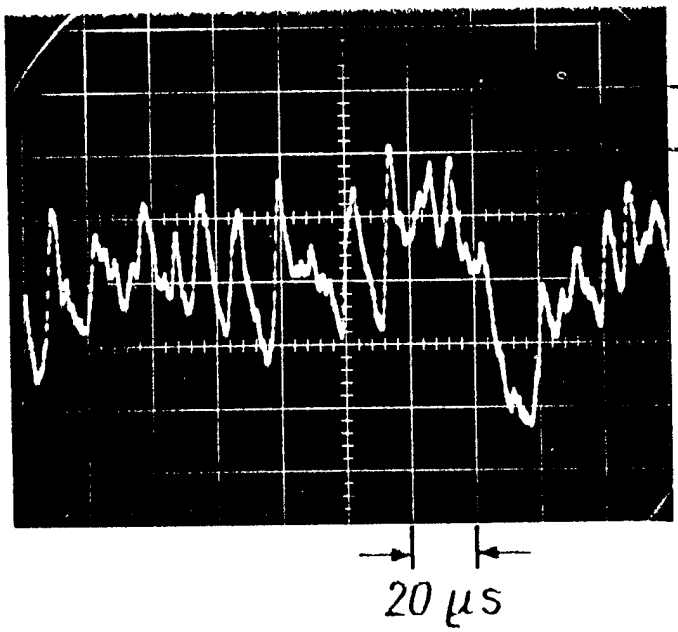

Fig. 9

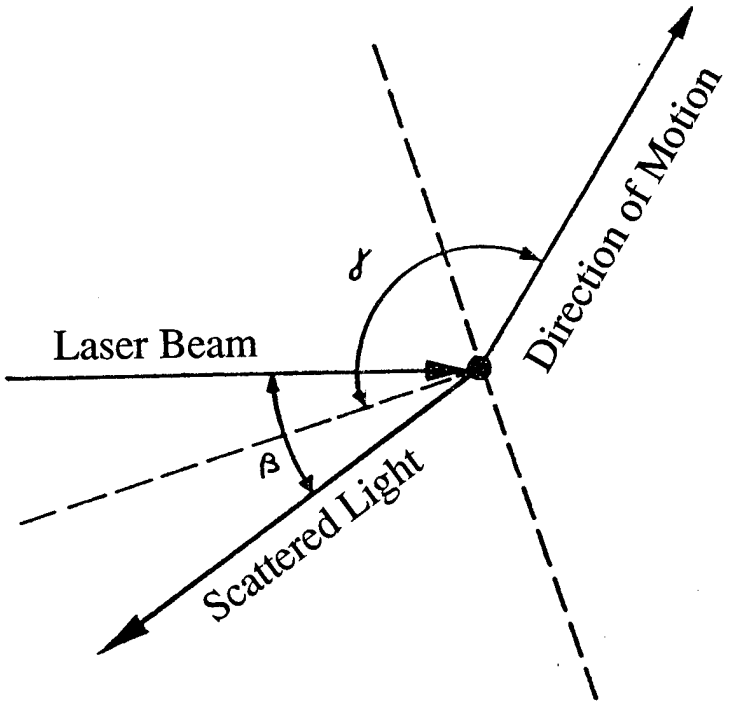

Fig. 10

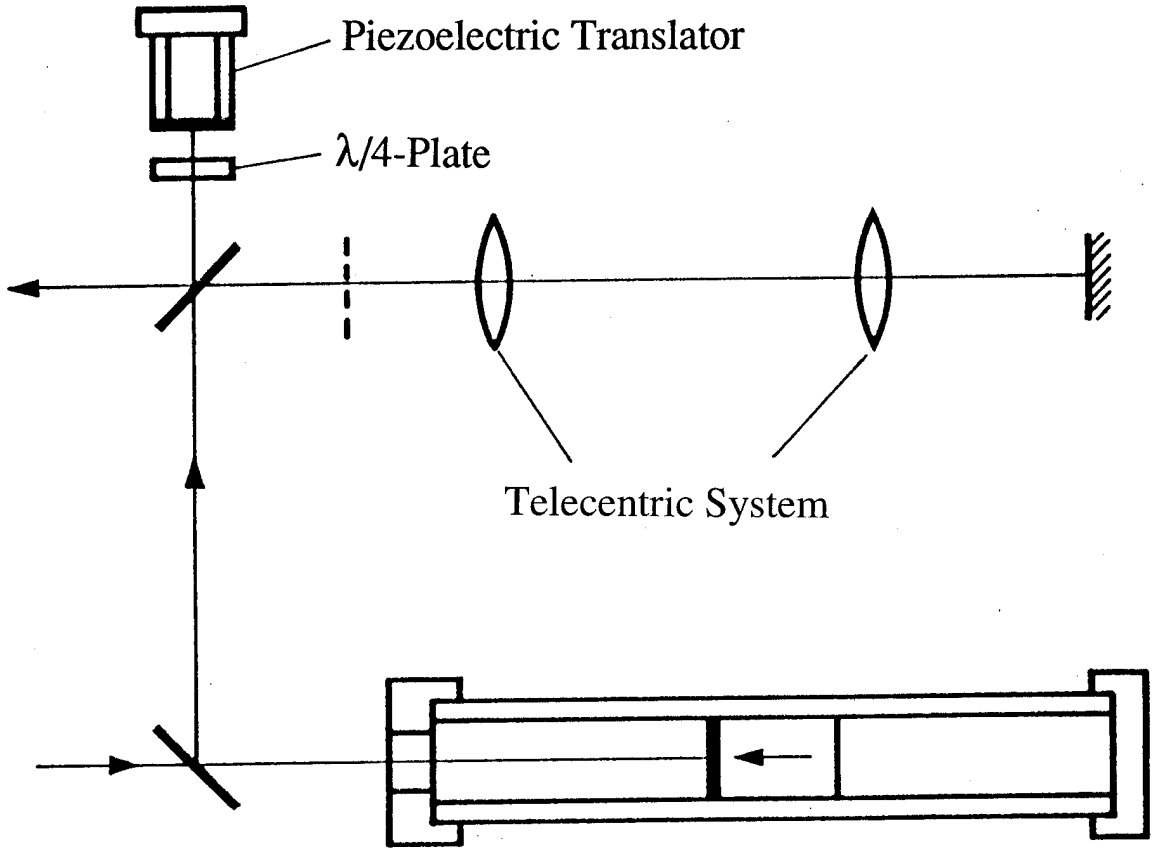
Piezoelectric Translator
λ/4-Plate
Telecentric System

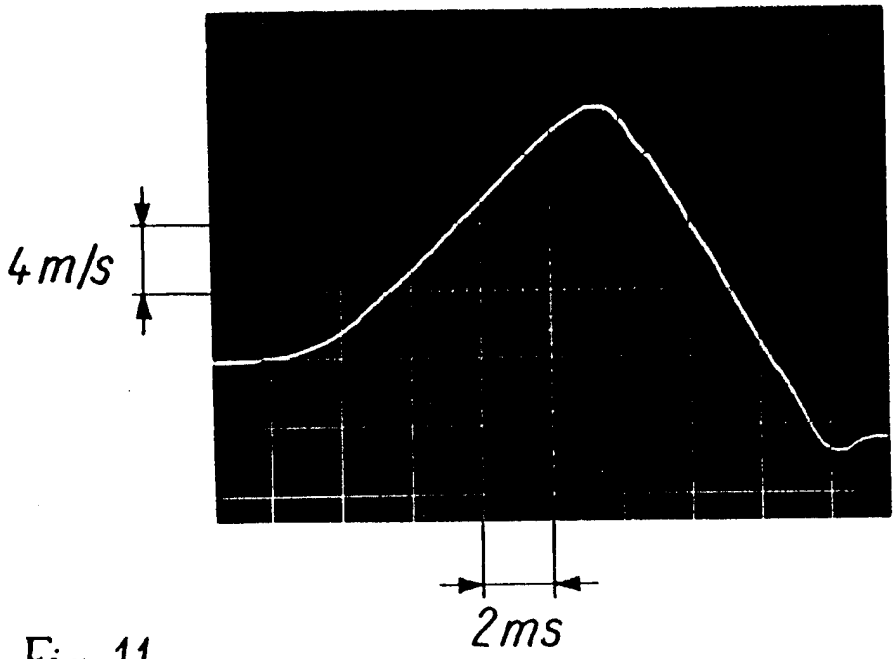
4 m/s
2 ms

Fig. 11

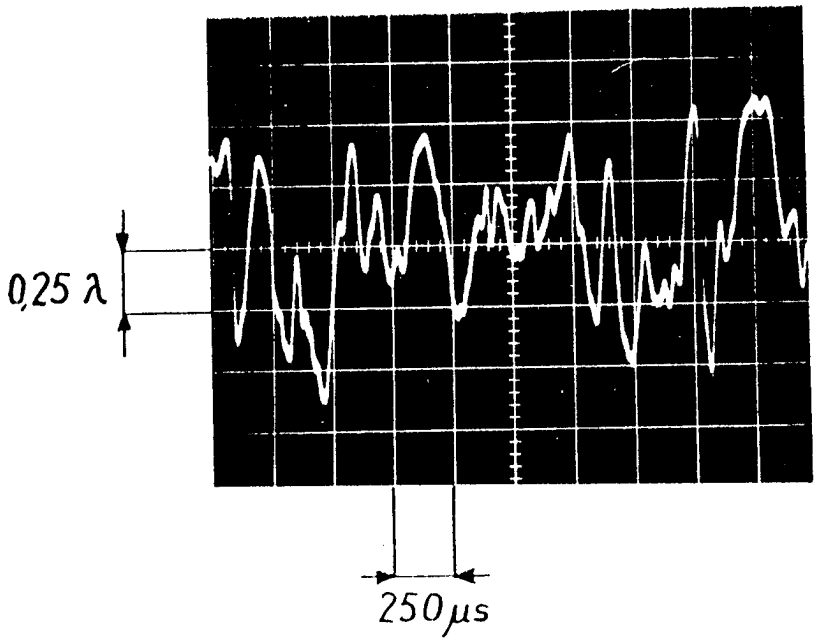

Fig. 12

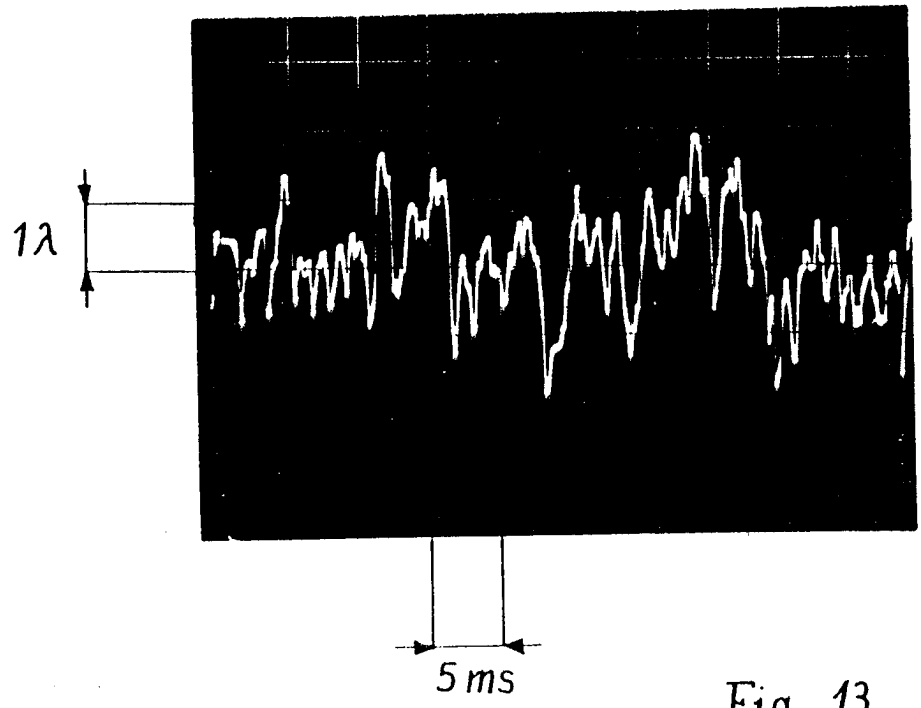

Fig. 13